

Accelerated MRSI Using Randomly Undersampled Spiral-Based k-Space Trajectories

Itthi Chatnuntawech¹, Borjan Gagoski², Berkin Bilgic³, Stephen Cauley³, Ellen Grant², Kawin Setsompop^{3,4}, and Elfar Adalsteinsson^{1,5}

¹MIT, Cambridge, MA, United States, ²Fetal-Neonatal Neuroimaging & Developmental Science Center, MA, United States, ³A. A. Martinos Center for Biomedical Imaging, MA, United States, ⁴Harvard Medical School, MA, United States, ⁵Harvard-MIT Health Sciences and Technology, Institute of Medical Engineering & Science, MA, United States

TARGET AUDIENCE: MRSI investigators, Image reconstruction scientists.

PURPOSE: We present an acquisition-reconstruction method (**random SENSE+TV**) to accelerate MRSI by random undersampling of k-space data, while maintaining acceptable reconstruction quality as measured by a normalized root-mean-square error (RMSE) of the reconstructed metabolite maps. Random SENSE+TV yields lower RMSEs of metabolite maps compared to other methods with the same scan time and is able to achieve a factor of 4.5 acceleration with the same reconstruction quality as the fully-sampled data.

METHODS: Uniformly undersampled spiral acquisition¹ uses spiral trajectories with fixed radius and undersamples by uniformly skipping interleaves. In contrast, random SENSE+TV uses spiral trajectories with different radii to randomly undersample the data in (k_x , k_y , k_t) space (Fig 1)². Sensitivity encoding technique (SENSE)³ with total variation (TV) regularization is used for

reconstruction as in: $\min_{\mathbf{x}_{cart}} \sum_i^{N_{channel}} \left\| \mathbf{A}_{cart2spiral} \mathbf{F}_\Omega \mathbf{C}_i \mathbf{x}_{cart} - \mathbf{y}_{spiral_i} \right\|_2^2 + \lambda TV(\mathbf{x}_{cart})$, where

$\mathbf{x}_{cart}(x, y, f)$ is the reconstructed Cartesian data, \mathbf{y}_{spiral_i} is the observed non-Cartesian k-space data from the i^{th} coil, \mathbf{C}_i is the sensitivity of the i^{th} coil, \mathbf{F}_Ω is the undersampled Fourier transform, $\mathbf{A}_{cart2spiral}$ is the 3D Cartesian-to-spiral operator, $TV(\cdot)$ is the total variation operator, λ is a regularization parameter. We demonstrated the feasibility of random SENSE+TV on a healthy volunteer with single-slice (1-cm thick) MRSI acquired fully-sampled at 3T and then retrospectively undersampled. Full sampling used 6 angular and 2 temporal interleaves, voxel size 0.56 cc, $FOV_{xy} = 24\text{cm} \times 24\text{cm}$, 32×32 voxels, 320 k_t points over a readout duration of 320 ms with spectral bandwidth of 1kHz. The PRESS excitation ($9 \times 9 \times 1$ cm) was positioned entirely within the head. The water component was suppressed using both chemical shift selective imaging (CHESS)⁴ and additional spectrally selective water suppression pulses. TR and TE were 1.8 s and 87 ms. Lipids were suppressed using the outer volume suppression (OVS)⁵. Eight different spiral trajectories were used to achieve $R=3$ and $R=6$. The duration of the spirals was in a range from 0.47ms to 2ms. Two comparisons were made. First, we compared the RMSEs of reconstructed metabolite maps from four acquisition-reconstruction methods with the same scan time. The methods included fully-sampled (but fewer number of averages to match the scan time of other methods), denoised fully-sampled (using a Schatten 1-norm regularization⁶), TV-regularized SENSE reconstruction with a uniformly undersampled spiral acquisition (uniform SENSE+TV), and random SENSE+TV. We acquired 50-averages ($N_{avg} = 50$), fully-sampled ($R = 1$), non-Cartesian MRSI data in 18 minutes, reconstructed with SENSE, and used the reconstructed data as (low noise) ground truth. Second, we compared the acquisition time required for the fully-sampled data and random SENSE+TV to achieve the same RMSE of the reconstructed NAA map to determine how much we can accelerate MRSI using random SENSE+TV.

RESULTS: For the first comparison, at $R=3$ (shown in Fig 2), the fully-sampled, denoised fully-sampled, uniform SENSE+TV, and random SENSE+TV methods yielded (27.5, 24.1, 27.2)%, (7.8, 12.7, 14.1)%, (13.0, 11.2, 12.2)%, and (6.8, 9.3, 9.8)% RMSE for the reconstructed (NAA, Cr, Cho) maps, respectively. At $R=6$, the fully-sampled, denoised fully-sampled, uniform SENSE+TV, and random SENSE+TV methods yielded (54.0, 44.3, 57.0)%, (10.6, 15.4, 17.0)%, (18.1, 21.5, 27.0)%, and (11.2, 12.1, 12.1)% RMSE for the reconstructed (NAA, Cr, Cho) maps, respectively. For the second comparison, random SENSE+TV with an acquisition time of 1.44 minutes yielded the same RMSE of the reconstructed NAA map as the fully-sampled data with an acquisition time of 6.48 minutes.

DISCUSSION: Random SENSE+TV generally yielded lowest RMSEs of the reconstructed maps, compared to other methods with the same scan time. Random SENSE+TV improves the reconstruction quality by undersampling not only in (k_x , k_y) space, but also along the k_t axis, which introduces artifacts that are less-structured. Further, random SENSE+TV imposes a prior knowledge on the structure of the data, which improves the condition of the problem. Limitations in this study include that the undersampling that was done retrospectively in MATLAB. Future work includes extensions to full-brain coverage and incorporation of modeling⁷⁻¹⁰ for strong subcutaneous lipids.

CONCLUSION: As demonstrated through in vivo results, random SENSE+TV reduces RMSEs of metabolite maps compared to other methods with the same scan time. Furthermore, by using random SENSE+TV, a factor of 4.5 acceleration is achievable while keeping equivalent reconstruction quality as the fully-sampled data, as measured by the RMSE of reconstructed NAA maps.

REFERENCES:

- [1] Eslami et al. IEEE ISBI (2011); [2] Gagoski et al. ISMRM (2012); [3] Pruessmann et al. MRM (1999); [4] Haase et al. PMB (1985); [5] Duyn et al. Radiology (1993); [6] Nguyen et al. MRM (2013); [7] Eslami et al. IEEE TMI (2010); [8] Bao et al. IEEE TMI (2007); [9] Bhavet et al. MRM (2013); [10] Bilgic et al. MRM (2012);

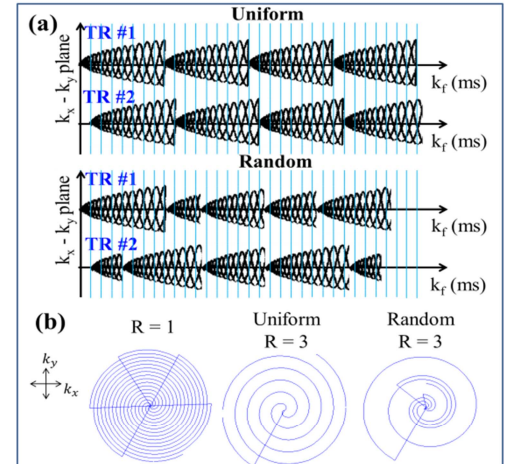


FIG. 1. (a) Two types of spiral-based k-space acquisition schemes: uniformly (top) and randomly (bottom) undersampled acquisition schemes. (b) The projections of possible k-space trajectories onto the k_x - k_y plane. The projection from fully-sampled, uniformly undersampled ($R=3$), and randomly undersampled ($R=3$) acquisitions are shown from left to right, respectively.

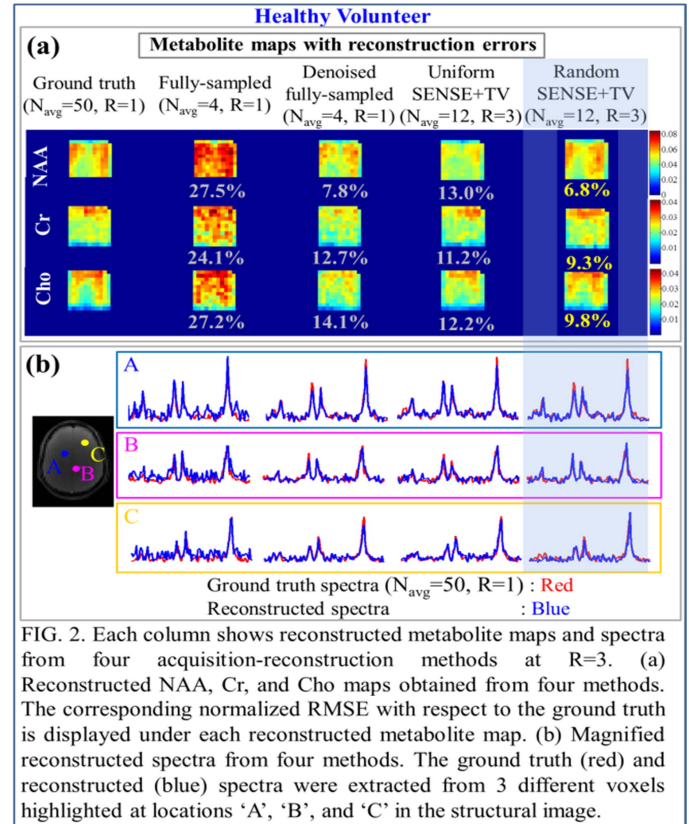


FIG. 2. Each column shows reconstructed metabolite maps and spectra from four acquisition-reconstruction methods at $R=3$. (a) Reconstructed NAA, Cr, and Cho maps obtained from four methods. The corresponding normalized RMSE with respect to the ground truth is displayed under each reconstructed metabolite map. (b) Magnified reconstructed spectra from four methods. The ground truth (red) and reconstructed (blue) spectra were extracted from 3 different voxels highlighted at locations 'A', 'B', and 'C' in the structural image.